# Crystallographic snapshots of sulfur insertion by lipoyl synthase

Martin I. McLaughlin[a,b,1], Nicholas D. Lanz[c], Peter J. Goldman[a], Kyung-Hoon Lee[b], Squire J. Booker[b,c,d], and Catherine L. Drennan[a,e,f,2]

[a]Department of Chemistry, Massachusetts Institute of Technology, Cambridge, MA 02139; [b]Department of Chemistry, The Pennsylvania State University, University Park, PA 16802; [c]Department of Biochemistry and Molecular Biology, The Pennsylvania State University, University Park, PA 16802; [d]Howard Hughes Medical Institute, The Pennsylvania State University, University Park, PA 16802; [e]Department of Biology, Massachusetts Institute of Technology, Cambridge, MA 02139; and [f]Howard Hughes Medical Institute, Massachusetts Institute of Technology, Cambridge, MA 02139

Edited by Vern L. Schramm, Albert Einstein College of Medicine, Bronx, NY, and approved July 5, 2016 (received for review March 8, 2016)

**Lipoyl synthase (LipA) catalyzes the insertion of two sulfur atoms at the unactivated C6 and C8 positions of a protein-bound octanoyl chain to produce the lipoyl cofactor. To activate its substrate for sulfur insertion, LipA uses a [4Fe-4S] cluster and *S*-adenosylmethionine (AdoMet) radical chemistry; the remainder of the reaction mechanism, especially the source of the sulfur, has been less clear. One controversial proposal involves the removal of sulfur from a second (auxiliary) [4Fe-4S] cluster on the enzyme, resulting in destruction of the cluster during each round of catalysis. Here, we present two high-resolution crystal structures of LipA from *Mycobacterium tuberculosis*: one in its resting state and one at an intermediate state during turnover. In the resting state, an auxiliary [4Fe-4S] cluster has an unusual serine ligation to one of the irons. After reaction with an octanoyllysine-containing 8-mer peptide substrate and 1 eq AdoMet, conditions that allow for the first sulfur insertion but not the second insertion, the serine ligand dissociates from the cluster, the iron ion is lost, and a sulfur atom that is still part of the cluster becomes covalently attached to C6 of the octanoyl substrate. This intermediate structure provides a clear picture of iron–sulfur cluster destruction in action, supporting the role of the auxiliary cluster as the sulfur source in the LipA reaction and describing a radical strategy for sulfur incorporation into completely unactivated substrates.**

iron–sulfur cluster | radical SAM enzyme | lipoic acid

The functionalization of aliphatic carbon centers is widely regarded as one of the most kinetically challenging reactions in nature, a striking example of which is found in the biosynthesis of the lipoyl cofactor, famous for its central role as the "swinging arm" of the pyruvate dehydrogenase enzyme complex. Lipoyl synthase (LipA) generates the lipoyl cofactor by insertion of two sulfur atoms at C6 and C8 of a protein-bound *n*-octanoyl chain, sites distal from the nearest functionality (1–4). LipA and the closely related biotin synthase (BioB) (Scheme 1) are founding members of the ever-expanding *S*-adenosyl-L-methionine (AdoMet) radical enzyme superfamily that uses a [4Fe-4S] cluster to reductively cleave the C5′-S bond of AdoMet, generating methionine and a 5′-deoxyadenosyl radical (5′-dA•), a powerful oxidant (5, 6). LipA requires 2 eq AdoMet—one per sulfur insertion—and two sulfur atoms to produce 1 eq lipoyl product through radical-based chemistry (4). One of the most controversial aspects of the LipA and BioB reactions is the source of the sulfur. AdoMet radical enzymes that catalyze sulfur insertion always seem to have an additional iron–sulfur (Fe/S) cluster: a [2Fe-2S] cluster in BioB (7), a [4Fe-4S] cluster in LipA (8), and a [4Fe-4S] cluster in the methylthiotransferases RimO and MiaB (9, 10). These auxiliary clusters in LipA and BioB have been proposed to be cannibalized during turnover to supply the inserted sulfur atom(s) (8, 11–13), a proposal that has not enjoyed universal agreement. Here, we investigate this incredible sulfur insertion chemistry through crystallographic snapshots of LipA from the human pathogen *Mycobacterium tuberculosis* both in the absence of substrate and at an intermediate stage in the reaction, just after insertion of the C6 sulfur atom but before sulfur insertion at C8.

## Results

The crystal structure of LipA from *M. tuberculosis* was determined to 1.64-Å resolution by iron multiwavelength anomalous dispersion phasing (Table S1). The overall fold of LipA consists of a $(\beta/\alpha)_6$ partial barrel common to most AdoMet radical enzymes (14), an N-terminal α-helical extension, and a C-terminal extension (Fig. 1*A* and Fig. S1). The [4Fe-4S] cluster that binds AdoMet and is responsible for radical generation is coordinated by three cysteines of the $CX_3CX\Phi C$ motif (Φ denotes an aromatic residue) that is on the AdoMet radical loop between β1 and α1 of the barrel (Fig. S2). The second (auxiliary) [4Fe-4S] cluster is sandwiched between the N- and C-terminal extensions (Fig. 1*A*). As also observed in a recent structure of LipA from *Thermosynechococcus elongatus* (15), three of the iron ions of the auxiliary cluster are ligated by cysteines residing in a conserved N-terminal $CX_4CX_5C$ motif, whereas the fourth iron ion is ligated by S292 found in a conserved C-terminal R(S/T)SΦ motif (Fig. 1*B* and Fig. S1). R290 of this R(S/T)SΦ motif extends between the two [4Fe-4S] clusters and covers the most exposed face of the auxiliary cluster with the aliphatic portion of its side

### Significance

**Lipoic acid, an enzyme cofactor in central metabolism and a livestock feed supplement, is produced on an industrial scale by a costly multistep synthesis. Nature makes lipoic acid in one step by the chemically challenging addition of two sulfur atoms to an inert fatty acid chain. The sulfur source in this reaction has been controversial, and its identity has implications for engineering microorganisms to overproduce lipoic acid. Structural characterization of a lipoyl synthase enzyme captured in the middle of catalysis shows unequivocally that the enzyme obtains its sulfur atoms by cannibalizing an iron–sulfur cluster, another ancient and essential cofactor. This result reveals an alternative strategy for sulfur mobilization and an unexpected self-sacrificial role for iron–sulfur clusters in biology.**

Author contributions: M.I.M., N.D.L., S.J.B., and C.L.D. designed research; M.I.M., N.D.L., P.J.G., and K.-H.L. performed research; N.D.L. and K.-H.L. contributed new reagents/analytic tools; M.I.M., N.D.L., P.J.G., S.J.B., and C.L.D. analyzed data; and M.I.M., N.D.L., P.J.G., S.J.B., and C.L.D. wrote the paper.

The authors declare no conflict of interest.

This article is a PNAS Direct Submission.

Data deposition: The atomic coordinates and structure factors have been deposited in the Protein Data Bank, www.wwpdb.org (PDB ID codes 5EXI, 5EXJ, and 5EXK).

[1]Present address: Department of Chemistry, University of Illinois at Urbana–Champaign, Urbana, IL 61801.

[2]To whom correspondence should be addressed. Email: cdrennan@mit.edu.

This article contains supporting information online at www.pnas.org/lookup/suppl/doi:10.1073/pnas.1602486113/-/DCSupplemental.

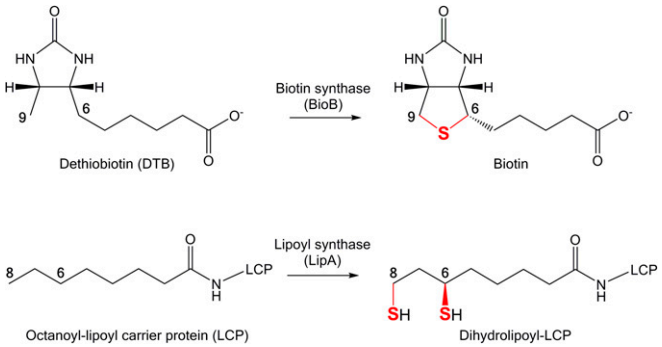


**Scheme 1.** The reactions catalyzed by the AdoMet radical sulfur insertion enzymes (*Upper*) BioB and (*Lower*) LipA. The inserted sulfur atoms are marked in red.

chain (Fig. 1*B*). In the absence of substrate, the active site is open and filled with solvent, with a 15.3-Å distance between the two clusters (Fig. 2*A*). Thus, for the auxiliary cluster to serve as the source of sulfur, displacement of R290 and a conformational tightening of the active site seem to be required.

To investigate the mechanism of sulfur insertion by LipA, we crystallographically characterized a stable but kinetically competent reaction intermediate that was previously described by Lanz et al. (16) for *Escherichia coli* LipA. Briefly, MtLipA was reacted with a synthetic peptide corresponding to eight residues of the *M. tuberculosis* octanoyl-H protein (sequence $ESTK_{oct}SVSD$), which supports turnover at the same rate as the full-length protein (17), excess reductant, and 1 eq AdoMet (Scheme 2). Upon reaction under these conditions for 45 min, the resulting protein sample was crystallized, and the crystal structure was determined to 1.86-Å resolution. This "intermediate-bound" structure contains six molecules in the asymmetric unit, all bound with the peptide substrate as well as methionine and 5′-deoxyadenosine (5′-dA), the reductive cleavage products of AdoMet.

The substrate peptide binds primarily to the N-terminal extension of LipA, such that its octanoyllysine residue inserts into the cavity between the Fe/S clusters (Fig. 1*C*). It is held in place chiefly by hydrogen bonding contacts involving peptide backbone atoms (Fig. 3). Comparison of the substrate-free and intermediate-bound LipA structures shows a pronounced conformational rearrangement of the enzyme: the N-terminal extension and auxiliary cluster move toward the barrel core (Fig. 1 *A* and *C* and Fig. S3), closing off the active site to solvent and decreasing the distance between the clusters to 11.8 Å. Residues 4–30, disordered in the substrate-free structure, are now ordered with residues 4–18 forming a helix adjacent to the AdoMet radical loop and residues 19–35 connecting this helix to the rest of the N-terminal extension (Fig. 1*C*).

The loop in the C-terminal extension that contains the R(S/T)SΦ motif also has been rearranged, and R290 is no longer blocking substrate access to the auxiliary cluster (Fig. 1*D*). R290 now packs against the octanoyl moiety of the substrate and hydrogen bonds to its acyl carbonyl oxygen (Fig. 1*D*). The octanoyllysine is additionally secured through hydrogen bonds between its acyl amide and peptidyl amide nitrogens and the carbonyl oxygens of A58 and G59, respectively (Fig. 3), residues that are found in a highly conserved part of LipA sequences between the first and second cysteines of the auxiliary cluster $CX_4CX_5C$ motif (Fig. S2). Through these interactions, octanoyllysine appears beautifully positioned for radical-based sulfur insertion, in that Met, 5′-dA, and the octanoyl group are all buried away from solvent and all within van der Waals distances of each other (Fig. 2*B*, Fig. S4, and Table S2). In particular, the C5′ of 5′-dA, which performs the H• abstraction, is 4.2 Å from C6 of the octanoyl substrate. Additionally, the orientation of the octanoyl group with respect to 5′-dA and the auxiliary cluster is consistent with the abstraction of the *pro*-R H• from C6 (2) and inversion of configuration on sulfur insertion (Fig. 2*B* and Fig. S4).

Consistent with the first half reaction having taken place, we find that the substrate octanoyl group is covalently attached to the auxiliary cluster by a bond between C6 and a cluster sulfur atom (Fig. 1*D*). S292 is no longer a ligand to the cluster, and the iron atom that was coordinated by S292 in the substrate-free structure is no longer present (Fig. 2*C*, *Inset*). Previously, a Mössbauer spectroscopic study revealed the loss of an iron atom from the auxiliary cluster on the timescale of the first sulfur insertion (16), and here, we see which iron is lost, and potentially, how it is lost: a solvent-filled cavity exists on one side of the cluster that extends to the protein surface (Fig. 2*C*). These structural data also present an explanation of why iron loss could be of mechanistic significance. The presence of this iron atom would block access of the two closest sulfur atoms of the auxiliary cluster (5.5 and 5.3 Å) to C8 of the octanoyl moiety (Fig. S4), hindering the second sulfur insertion.

## Discussion

The chemical difficulty of synthesizing the lipoyl and biotin cofactors cannot be overstated. This point is exemplified by the fact that 10–30 tons of biotin sold each year are produced by a chemical synthetic route that is estimated to have as many as 15 steps (18). First, the challenge of regio- and stereoselective C–H bond activation must be overcome, and second, a route for sulfur functionalization must be achieved. Here, we find that the LipA substrate is exquisitely positioned next to 5′-dA for *pro*-R H• abstraction, allowing for this requisite selectivity. The next step is sulfur functionalization (Scheme 2), which raises the controversial issue of whether an Fe/S cluster is really the source of sulfur. In this respect, the structure of BioB sets the stage, revealing an auxiliary [2Fe-2S] cluster with an atypical arginine ligation near

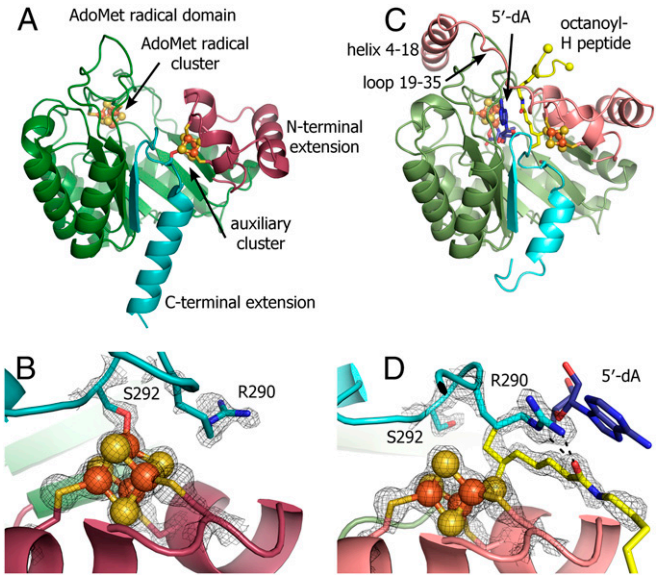


**Fig. 1.** Structural comparisons of substrate-free and intermediate-bound forms of LipA. (*A*) Structure of substrate-free LipA in ribbon representation with the $(\beta/\alpha)_6$ AdoMet radical domain (green), N-terminal extension (red), and C-terminal extension (blue). (*B*) The auxiliary [4Fe-4S] cluster of LipA in the absence of substrate. R290 and S292 of the R(S/T)SΦ motif are shown as sticks. Simulated annealing omit density ($2F_o-F_c$) is contoured at 2.0σ in black mesh. (*C*) Structure of LipA after reaction with 1 eq AdoMet in the presence of octanoyl-H peptide substrate (yellow); 5′-dA and methionine are in dark blue. A loop and helix comprising residues 4–30 become ordered when substrate is bound. (*D*) The auxiliary cluster of LipA with octanoyl-H peptide substrate (yellow) coordinated. Simulated annealing omit density ($2F_o-F_c$) is contoured at 2.0σ in black mesh.

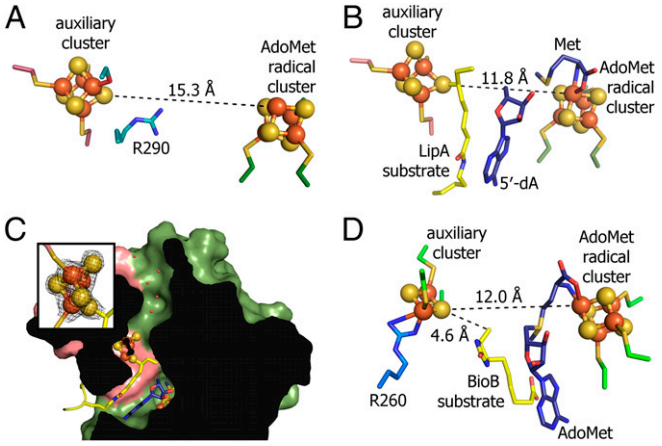


**Fig. 2.** The active sites of LipA and BioB. (*A*) Substrate-free LipA with R290 blocking access to auxiliary cluster. (*B*) Intermediate-bound LipA structure. (*C*) A cross-section of the intermediate-bound LipA structure showing water-filled cavity created by residues in β1 (E71–T73), β2 (Y117–T119), and the C-terminal helix (S292–R297). *Inset* depicts simulated annealing omit density ($2F_o–F_c$) around the auxiliary cluster contoured at 2.0σ. (*D*) BioB active site (Protein Data Bank ID code 1R30) with a highly conserved arginine residue, R260, ligating the auxiliary [2Fe-2S] cluster. AdoMet ligates the AdoMet radical cluster, whereas dethiobiotin, the substrate, is between AdoMet and the auxiliary cluster.

the substrate binding site and the radical AdoMet cluster (Fig. 2*D*) (19). In this work, we find that substrate binding to LipA induces a large conformational change that shortens the distance between Fe/S clusters (15.3–11.8 Å), such that the agreement with the substrate-bound structure of BioB is now incredible (Fig. 2 *B* and *D*). This consistent ∼12-Å distance seems to be ideal for substrate to be packed sufficiently close to the 5′-dA radical for H• abstraction and simultaneously near enough to the auxiliary cluster for sulfur insertion (4.6 Å in BioB). Interestingly, like BioB, there is an unusual ligand to the auxiliary cluster, but the ligand is a serine, not an arginine as it is in BioB. As far as we know, LipA is the only example of serine ligation to a [4Fe-4S] cluster in a WT protein. Serine ligands have been introduced into proteins with [4Fe-4S] clusters by mutagenesis, usually resulting in decreased cluster stability under oxidizing or acidic conditions (20–23). This latter property perhaps explains the choice of serine as a ligand for a [4Fe-4S] cluster that must be labile by design. Although it is not a ligand, arginine 290 of the R(S/T)SΦ motif seems critical for both protection of the auxiliary cluster in the absence of substrate and substrate binding.

Although [3Fe-4S] clusters are often found as dead-end products of oxidative inactivation of [4Fe-4S] enzymes, in LipA, these clusters seem to be reaction intermediates. The strongest support for the catalytic relevance of an intermediary [3Fe-4S] cluster comes from a Mössbauer spectroscopic study that showed that a [3Fe-4S] cluster appears and disappears on the timescale of LipA turnover (16). In particular, under the conditions used for these crystal trials (excess reductant and 1 eq AdoMet), *E. coli* LipA accumulates a cross-linked species that is stable to gel filtration chromatography and contains 0.9 eq monothiolated peptide and 0.6 eq 3-Fe–containing clusters (Scheme 2) with Mössbauer parameters similar to those of previously described [3Fe-4S] clusters. When reacted with excess AdoMet and reductant, this cross-linked species supports the formation of 0.5 eq lipoyl product in a kinetically competent manner, the Mössbauer signal for the 3-Fe–containing cluster

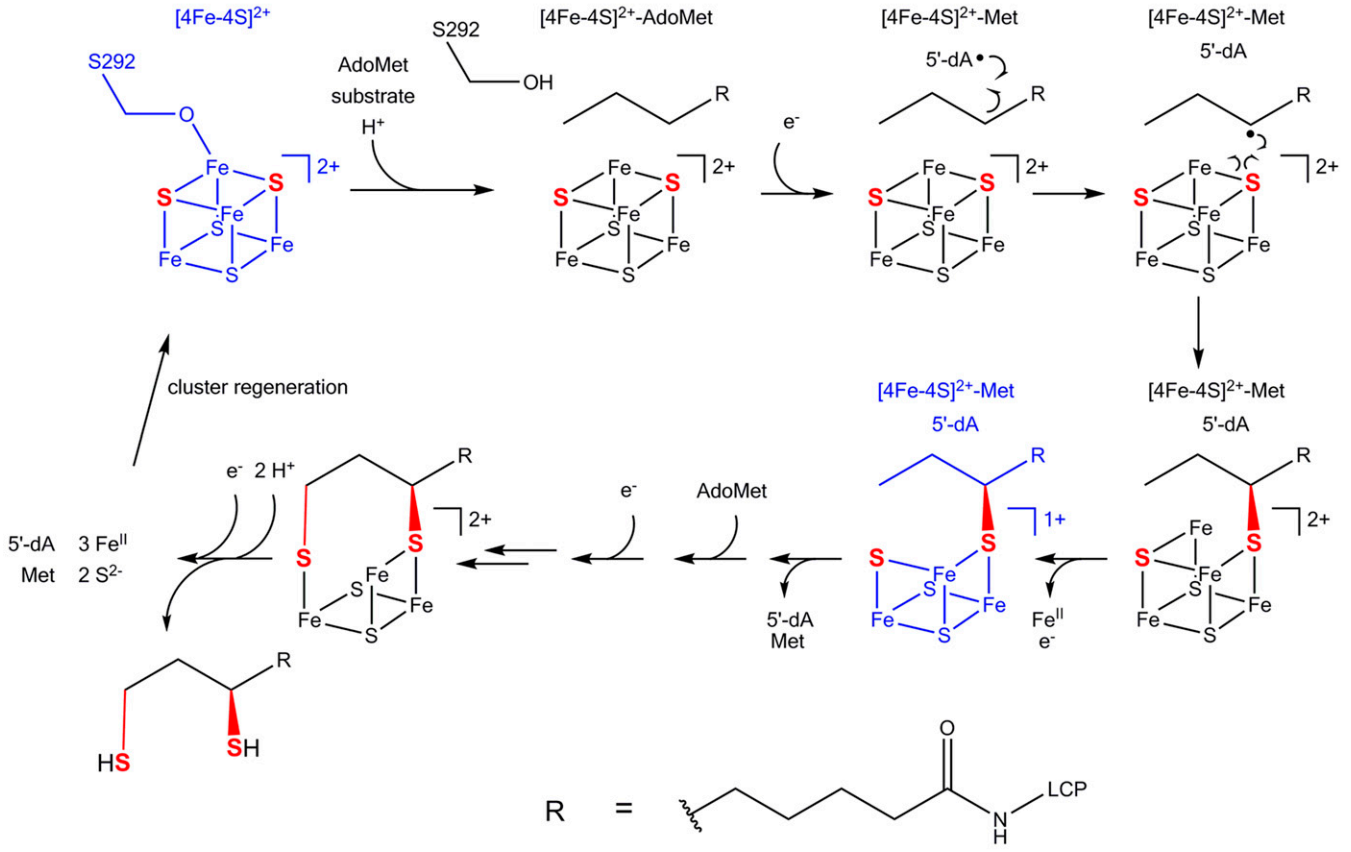


**Scheme 2.** Proposed catalytic mechanism for LipA. Inserted sulfur atoms are shown in red; species represented by the crystal structures described in the text are shown in blue. The timing of dissociation of the conserved serine ligand, S292, is unknown, but it is shown concomitant with substrate binding. Modified from ref. 16.

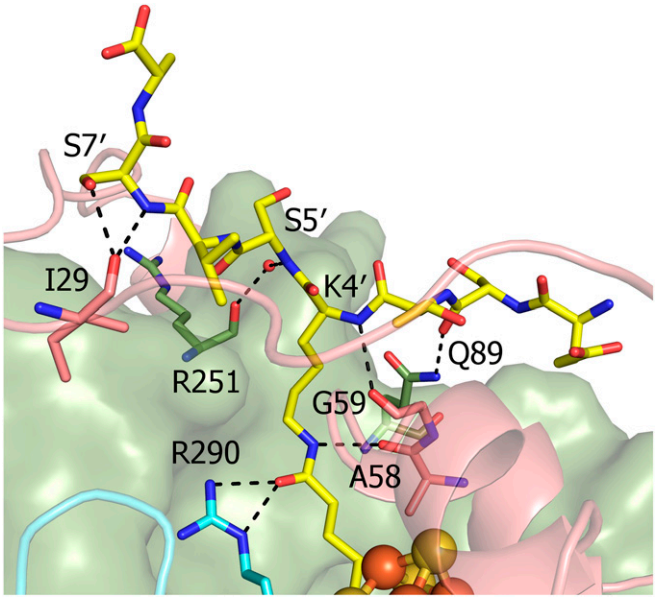


**Fig. 3.** Polar interactions between LipA and the octanoyl-H peptide substrate (yellow). Six chains are present in the crystal structure's asymmetric unit with various degrees of order; the interactions shown are only those present in four or more chains and mediated by zero or one water molecule. The N-terminal extension is in red, the AdoMet radical core is in green, and the C-terminal extension is in cyan.

disappears, and signals increase for N/O- and S-coordinated high-spin $Fe^{II}$, corresponding to degradation of the auxiliary cluster. For MtLipA, the analogous cross-linked species supports formation of almost a full equivalent of lipoyl product with a rate similar to that of the overall reaction (17).

One surprising attribute of the cross-linked intermediate is its unusual stability: over 5 d between intermediate generation and crystal growth and for an additional 4 d in crystallo, the partially degraded auxiliary cluster remains intact, and the peptide, 5′-dA, and methionine remain enzyme-bound. It stands to reason that LipA would maximize the sulfur yield from each Fe/S cluster by preventing dissociation of the monothiolated intermediate, but the persistence of 5′-dA and methionine is puzzling, considering that the second sulfur insertion requires their replacement with AdoMet for 5′-dA• generation. Attempts to soak a second molecule of AdoMet into crystals of the LipA intermediate (5 mM AdoMet for 5 d and 10 mM AdoMet for 1 d) do not displace 5′-dA and Met, suggesting that exchange may require a conformational change that is not possible in the crystal. However, cocrystallization of the intermediate-bound species with up to 5 mM AdoMet over several days also fails to exchange 5′-dA and Met for AdoMet, instead producing identical intermediate-bound crystals. These results may indicate that the AdoMet-bound intermediate complex does not crystallize as readily as the 5′-dA and Met-bound complex, that the exchange of 5′-dA and Met for AdoMet is highly unfavorable, or that the dissociation of 5′-dA and Met is slow. Although current data do not support any one explanation, if either of the latter two explanations is correct, exchange may be at least partially rate-limiting in solution-phase experiments with MtLipA.

Overall, these structures corroborate previous biochemical and spectroscopic studies on LipA (3, 4, 8, 13, 16, 17) and support the role of the auxiliary cluster as the sulfur donor (Scheme 2). By showing the octanoyllysine moiety covalently attached to a sulfur atom in the auxiliary cluster, these structural data represent a smoking gun for what has been a truly heated debate about the sulfur source for these reactions. Although these structures may end this debate, there are many exciting questions about LipA that remain: after the first sulfur insertion, how are 5′-dA and Met exchanged for a second equivalent of AdoMet, and which of the two equidistant sulfur atoms is inserted into C8? Perhaps the most enigmatic question regarding the LipA mechanism is the ultimate fate of the degraded auxiliary cluster in vivo. It may be repaired on LipA, removed and replaced by Fe/S cluster assembly machinery, or simply released in the form of free iron and inorganic sulfide ions. The latter process would seem to present a problem for the cell in the form of iron and sulfide toxicity. Given that LipA enzymes exist in a wide range of organisms from pathogens to humans, it is unclear whether there will be a single solution to this question. Certainly, the sulfur insertions en route to production of the lipoyl and biotin cofactors will continue to fascinate for years to come.

## Materials and Methods

N-terminally $His_6$-tagged MtLipA was expressed in *E. coli* BL21(DE3) cells, purified under anaerobic conditions, and reconstituted with iron and sulfide as described previously (16, 17). The MtLipA intermediate was generated by reaction of 200 μM as-isolated MtLipA with 300 μM octanoyl substrate peptide, 180 μM AdoMet, and 2 mM sodium dithionite anaerobically at room temperature for 45 min; intermediate formation was monitored by liquid chromatography-MS of acid-quenched reaction samples (*SI Materials and Methods*). MtLipA and the MtLipA intermediate were crystallized anaerobically by the vapor diffusion method. Each structure was solved from data collected on a single crystal at beamline ID-C of the Advanced Photon Source. The structure of MtLipA alone was originally solved to 2.28-Å resolution by Fe multiwavelength anomalous dispersion; later, a higher-resolution dataset was collected from a different crystal, and a second structure was solved to 1.64-Å resolution using the first structure as a search model for molecular replacement. This high-resolution MtLipA structure was used as a molecular replacement model to solve the intermediate-bound structure. Details of crystallization, data collection, structure solution, model building, and refinement can be found in *SI Materials and Methods*.

**ACKNOWLEDGMENTS.** This work was supported by NIH Grants R01GM063847 (to S.J.B.) and R01GM103268 (to S.J.B.) and National Science Foundation Grant MCB-0543833 (to C.L.D.). Additionally, C.L.D. and S.J.B. are Howard Hughes Medical Investigators. Additional funding was provided by the Meryl and Stewart Robertson Undergraduate Research Opportunities Program Fund, the Massachusetts Institute of Technology Energy Initiative, and the DeFlorez Endowment Fund. This work is based on research conducted at the Advanced Photon Source (APS) on the Northeastern Collaborative Access Team beamlines, which are supported by National Institute of General Medical Sciences Grant P41GM103403. Use of the APS, an Office of Science User Facility operated for the US Department of Energy (DOE), was supported by US DOE Contract DE-AC02-06CH11357.

1. Miller JR, et al. (2000) *Escherichia coli* LipA is a lipoyl synthase: In vitro biosynthesis of lipoylated pyruvate dehydrogenase complex from octanoyl-acyl carrier protein. *Biochemistry* 39(49):15166–15178.
2. White RH (1980) Stable isotope studies on the biosynthesis of lipoic acid in *Escherichia coli*. *Biochemistry* 19(1):15–19.
3. Douglas P, Kriek M, Bryant P, Roach PL (2006) Lipoyl synthase inserts sulfur atoms into an octanoyl substrate in a stepwise manner. *Angew Chem Int Ed Engl* 45(31):5197–5199.
4. Cicchillo RM, et al. (2004) Lipoyl synthase requires two equivalents of *S*-adenosyl-L-methionine to synthesize one equivalent of lipoic acid. *Biochemistry* 43(21):6378–6386.
5. Lieder KW, et al. (1998) *S*-Adenosylmethionine-dependent reduction of lysine 2,3-aminomutase and observation of the catalytically functional iron-sulfur centers by electron paramagnetic resonance. *Biochemistry* 37(8):2578–2585.
6. Frey PA, Hegeman AD, Ruzicka FJ (2008) The radical SAM superfamily. *Crit Rev Biochem Mol Biol* 43(1):63–88.
7. Cosper MM, et al. (2004) Characterization of the cofactor composition of *Escherichia coli* biotin synthase. *Biochemistry* 43(7):2007–2021.
8. Cicchillo RM, et al. (2004) *Escherichia coli* lipoyl synthase binds two distinct [4Fe-4S] clusters per polypeptide. *Biochemistry* 43(37):11770–11781.
9. Hernández HL, et al. (2007) MiaB, a bifunctional radical-*S*-adenosylmethionine enzyme involved in the thiolation and methylation of tRNA, contains two essential [4Fe-4S] clusters. *Biochemistry* 46(17):5140–5147.
10. Lee K-H, et al. (2009) Characterization of RimO, a new member of the methylthiotransferase subclass of the radical SAM superfamily. *Biochemistry* 48(42):10162–10174.
11. Bui BT, et al. (1998) Biotin synthase mechanism: On the origin of sulphur. *FEBS Lett* 440(1-2):226–230.

12. Ugulava NB, Sacanell CJ, Jarrett JT (2001) Spectroscopic changes during a single turnover of biotin synthase: Destruction of a [2Fe-2S] cluster accompanies sulfur insertion. *Biochemistry* 40(28):8352–8358.
13. Cicchillo RM, Booker SJ (2005) Mechanistic investigations of lipoic acid biosynthesis in *Escherichia coli*: Both sulfur atoms in lipoic acid are contributed by the same lipoyl synthase polypeptide. *J Am Chem Soc* 127(9):2860–2861.
14. Dowling DP, Vey JL, Croft AK, Drennan CL (2012) Structural diversity in the AdoMet radical enzyme superfamily. *Biochim Biophys Acta* 1824(11):1178–1195.
15. Harmer JE, et al. (2014) Structures of lipoyl synthase reveal a compact active site for controlling sequential sulfur insertion reactions. *Biochem J* 464(1):123–133.
16. Lanz ND, et al. (2014) Evidence for a catalytically and kinetically competent enzyme-substrate cross-linked intermediate in catalysis by lipoyl synthase. *Biochemistry* 53(28): 4557–4572.
17. Lanz ND, et al. (2016) Characterization of lipoyl synthase from *Mycobacterium tuberculosis*. *Biochemistry* 55(9):1372–1383.
18. De Clercq PJ (1997) Biotin: A timeless challenge for total synthesis. *Chem Rev* 97(6): 1755–1792.
19. Berkovitch F, Nicolet Y, Wan JT, Jarrett JT, Drennan CL (2004) Crystal structure of biotin synthase, an *S*-adenosylmethionine-dependent radical enzyme. *Science* 303(5654):76–79.
20. Calzolai L, et al. (1997) Solution NMR Study of the electronic structure and magnetic properties of cluster ligation mutants of the four-iron ferredoxin from the hyperthermophilic archaeon *Pyrococcus furiosus*. *J Am Chem Soc* 119(40):9341–9350.
21. Brereton PS, Duderstadt RE, Staples CR, Johnson MK, Adams MWW (1999) Effect of serinate ligation at each of the iron sites of the [$Fe_4S_4$] cluster of *Pyrococcus furiosus* ferredoxin on the redox, spectroscopic, and biological properties. *Biochemistry* 38(32):10594–10605.
22. Babini E, et al. (1996) A serine to cysteine ligand mutation in the high potential iron-sulfur protein from *Chromatium vinosum* provides insight into the electronic structure of the [4Fe-4S] cluster. *J Am Chem Soc* 118(1):75–80.
23. Mansy SS, et al. (2002) Crystal structure and stability studies of C77S HiPIP: A serine ligated [4Fe-4S] cluster. *Biochemistry* 41(4):1195–1201.
24. Iwig DF, Booker SJ (2004) Insight into the polar reactivity of the onium chalcogen analogues of *S*-adenosyl-L-methionine. *Biochemistry* 43(42):13496–13509.
25. Nesbitt NM, et al. (2005) Expression, purification, and physical characterization of *Escherichia coli* lipoyl(octanoyl)transferase. *Protein Expr Purif* 39(2):269–282.
26. Vonrhein C, Blanc E, Roversi P, Bricogne G (2007) Automated structure solution with autoSHARP. *Methods Mol Biol* 364:215–230.
27. Adams PD, et al. (2010) PHENIX: A comprehensive Python-based system for macromolecular structure solution. *Acta Crystallogr D Biol Crystallogr* 66(Pt 2):213–221.
28. Emsley P, Lohkamp B, Scott WG, Cowtan K (2010) Features and development of Coot. *Acta Crystallogr D Biol Crystallogr* 66(Pt 4):486–501.
29. Takeda K, Kusumoto K, Hirano Y, Miki K (2010) Detailed assessment of X-ray induced structural perturbation in a crystalline state protein. *J Struct Biol* 169(2):135–144.
30. Laskowski RA, MacArthur MW, Moss DS, Thornton JM (1993) PROCHECK: A program to check the stereochemical quality of protein structures. *J Appl Crystallogr* 26(Pt 2): 283–291.
31. Lovell SC, et al. (2003) Structure validation by Calpha geometry: $\varphi$, $\psi$ And Cbeta deviation. *Proteins* 50(3):437–450.